Resource

Cell Chemical Biology

Fluorescent RNA Aptamers as a Tool to Study RNA-Modifying Enzymes

Graphical Abstract

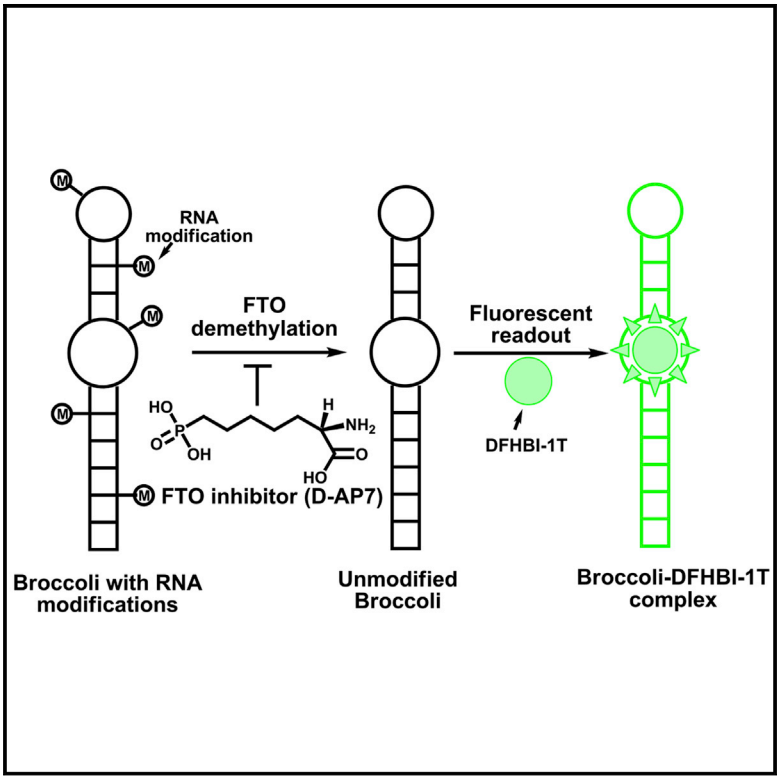

Authors

Nina Svensen, Samie R. Jaffrey

Correspondence

srj2003@med.cornell.edu

In Brief

RNA-modifying enzymes regulate diverse cellular RNAs but are difficult to assay. Svensen and Jaffrey describe the first fluorometric RNA substrates, based on the Broccoli RNA mimic of GFP. This approach enabled the discovery of novel inhibitors using a high-throughput screening approach.

Highlights

- High-throughput screening assay for RNA-modifying enzymes
- Broccoli RNA established as a fluorometric substrate for FTO and ALKBH5
- Identification of selective FTO inhibitors with novel structures
- In vivo inhibition of FTO regulates methylation levels in target mRNAs

Svensen & Jaffrey, 2016, Cell Chemical Biology *23*, 1–11
March 17, 2016
http://dx.doi.org/10.1016/j.chembiol.2015.11.018

CellPress

Please cite this article in press as: Svensen and Jaffrey, Fluorescent RNA Aptamers as a Tool to Study RNA-Modifying Enzymes, Cell Chemical Biology (2016), http://dx.doi.org/10.1016/j.chembiol.2015.11.018

Cell Chemical Biology
Resource

Fluorescent RNA Aptamers as a Tool to Study RNA-Modifying Enzymes

Nina Svensen[1] and Samie R. Jaffrey[1,*]
[1]Department of Pharmacology, Weill Cornell Medical College, Cornell University, New York, NY 10065, USA
*Correspondence: srj2003@med.cornell.edu
http://dx.doi.org/10.1016/j.chembiol.2015.11.018

SUMMARY

RNA-modifying enzymes are difficult to assay due to the absence of fluorometric substrates. Here we show that the Broccoli, a previously reported fluorescent RNA-dye complex, can be modified to contain N^6-methyladenosine, a prevalent mRNA base modification. Methylated Broccoli is nonfluorescent but, upon demethylation by the RNA demethylases fat mass and obesity-associated protein (FTO) or ALKBH5, it binds and activates the fluorescence of its cognate fluorophore. We describe a high-throughput screen (HTS) for FTO inhibitors using the fluorogenic methylated Broccoli substrate HTS assay, which performs robustly with a Z′ factor >0.8 in the LOPAC1280 library. This allowed the identification of novel high-affinity FTO inhibitors. Several of these compounds were selective for FTO over the related demethylase, ALKBH5, and increase methylation of endogenous FTO target mRNAs in cells. Lastly, we show that Broccoli can be modified to contain other base modifications, suggesting that this approach could be generally applicable for assaying diverse RNA-modifying enzymes.

INTRODUCTION

Numerous nucleotide modifications are introduced into RNA by diverse RNA-modifying enzymes (Limbach et al., 1994; Li and Mason, 2014). These RNA modifications exhibit remarkable chemical and structural diversity, with >100 different naturally occurring modified nucleosides identified (Limbach et al., 1994; Li and Mason, 2014). The modifications regulate many different cellular pathways and range from those with well-understood functions, to those with less well-understood functions (e.g., N^6-adenosine methylation and pseudouridylation) (Limbach et al., 1994; Li and Mason, 2014; Jaffrey, 2014).

RNA modifications and RNA-modifying enzymes are increasingly being linked to diseases (Umeda et al., 2005; McGuinness and McGuinness, 2014). Thus, RNA-modifying enzymes present a new set of potential drug targets. Importantly, this class of enzymes has not been targeted by conventional high-throughput screening (HTS) assays.

Establishing HTS assays for RNA-modifying enzymes is a major challenge. Current assays for detection of RNA modifications rely on high-performance liquid chromatography (HPLC) or mass spectrometry (MS), which can detect small changes to RNA, such as a single methyl group (Kowalak et al., 1993). Because these assays rely on HPLC and/or MS, they have low throughput (Barwick, 1999). Furthermore, detection of these RNA modifications requires degradation of the RNA to nucleosides, which requires two enzymatic steps (Kowalak et al., 1993). The requirement for coupled enzymatic steps greatly decreases the achievable Z′ factor in an HTS format (Barwick, 1999). These challenges make the current HPLC- and MS-based RNA-modifying enzyme assays poorly suited for HTS format.

A major approach for developing simple, sensitive, and specific assays of enzyme activity is the use of fluorometric substrates. These are substrates that are not fluorescent until they undergo a chemical reaction mediated by the enzyme of interest (Acker and Auld, 2014). Although fluorometric substrates are well established for other enzymes (Crespi et al., 2002; Palamakumbura and Trackman, 2002), fluorometric substrates have not been successfully developed for RNA-modifying enzymes. The challenge in developing fluorometric probes for RNA-modifying enzymes is that it is not clear how to couple enzymatic modification of a base to a change in fluorescence.

Here we describe a novel HTS approach to identify inhibitors of RNA-modifying enzymes, and the use of this assay to identify inhibitors of fat mass and obesity-associated protein (FTO), an enzyme that exhibits m^6A-demethylating activity (Jia et al., 2011). To measure FTO activity, we developed the first fluorometric RNA substrate that exhibits fluorescence in proportion to the activity of RNA-modifying enzymes. This RNA is based on the Broccoli RNA aptamer, which binds and activates the fluorescence of its cognate fluorophore, 3,5-difluoro-4-hydroxybenzylidene imidazolinone (DFHBI). We show that Broccoli synthesized with modified nucleotides, such as m^6A is nonfluorescent, but becomes fluorescent upon demethylation by FTO or ALKBH5. We use this assay to screen a compound library and identify novel potent FTO inhibitors. We show that some of these compounds are selective for FTO and enable modulation of RNA methylation levels in living cells. These data demonstrate the power of this generalizable approach for screening the activity of diverse RNA-modifying enzymes.

RESULTS

Effect of RNA Modifications on Broccoli-DFHBI-1T Fluorescence

We hypothesized that RNA base modifications could be detected when they are incorporated into RNAs that can form

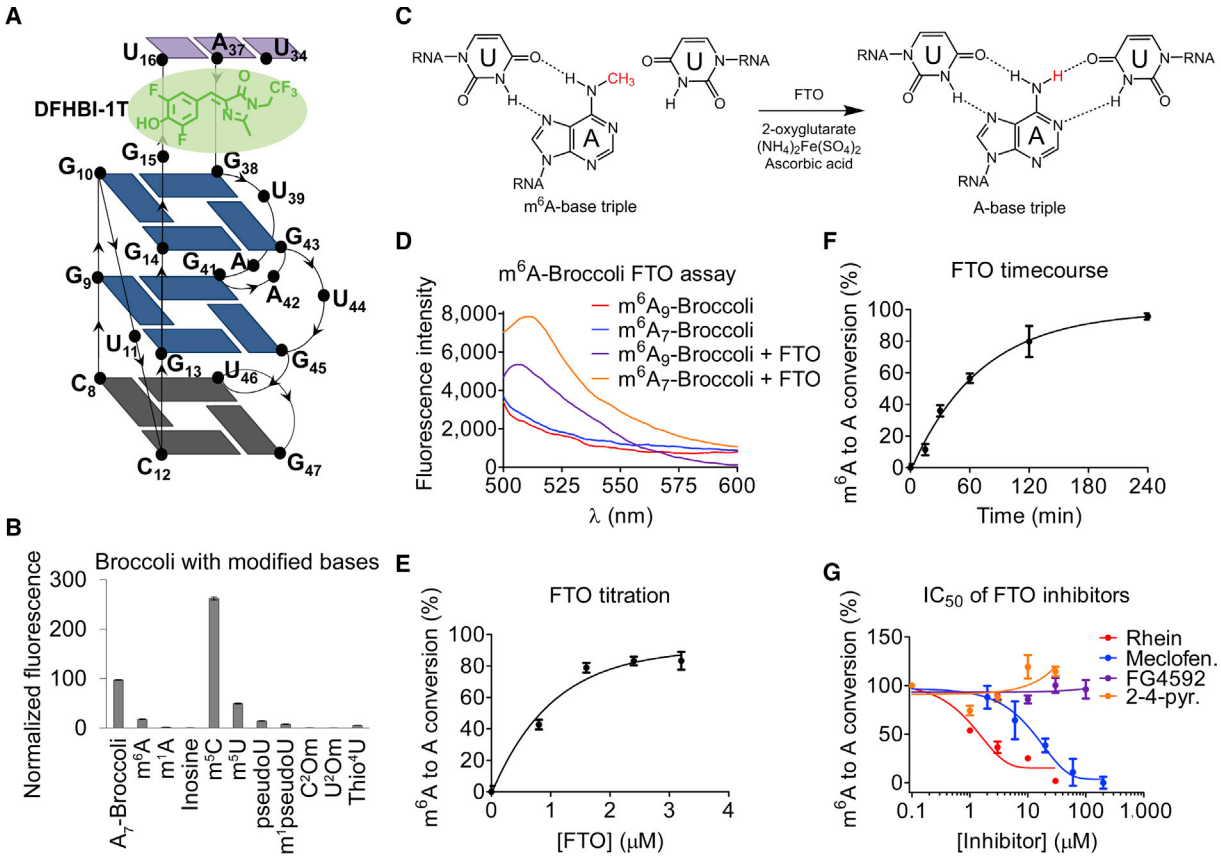

Figure 1. Application of m^{6}A-Modified Broccoli as a Fluorometric Substrate in the FTO Assay

(A) Core structure of the Broccoli-DFHBI-1T complex. DFHBI-1T (green) binds between the G-quadruplex (blue squares) and a base triple (purple squares). Grey squares indicate a tetrad below the G-quadruplexes.

(B) Effect of RNA modifications on Broccoli-DFHBI-1T fluorescence. To test whether RNA modifications affect the ability of Broccoli to bind and activate the fluorescence of DFHBI-1T, Broccoli was synthesized with the modified nucleotide in place of the wild-type base at every position. Data were normalized by background subtraction (DFHBI-1T buffer). m^n denotes base methylation in the n position of the ribonucleobase. ^{2}Om denotes 2′-*O*-methylation of the ribose.

(C) Scheme of FTO-catalyzed N^6-methyladenosine (m^{6}A) to adenosine-RNA conversion. m^{6}A is highlighted in red.

(D) m^{6}A-Broccoli is a fluorometric substrate for the FTO enzyme. The extent of FTO-catalyzed m^{6}A-Broccoli demethylation was measured using the fluorescence resulting from the A-Broccoli that is generated. m^{6}A$_9$-Broccoli (red line) or m^{6}A$_7$-Broccoli (blue line) were treated with FTO in a standard FTO assay. The amount of A$_9$-Broccoli-DFHBI-1T (purple line) and A$_7$-Broccoli-DFHBI-1T (orange line) fluorescence generated was measured following incubation with DFHBI-1T. Data were normalized by background subtraction (DFHBI-1T buffer).

(E) m^{6}A$_7$-Broccoli titrated with FTO. The extent of m^{6}A$_7$-Broccoli demethylation as a result of increasing FTO concentration was measured using the fluorescence resulting from A$_7$-Broccoli generation as readout. This assay was carried out as in (D) with increasing FTO concentration. Data were normalized to A$_7$-Broccoli control.

(F) FTO demethylation time course. The extent of FTO-catalyzed m^{6}A$_7$-Broccoli demethylation as a result of increasing time was measured using the fluorescence resulting from A$_7$-Broccoli generation as the readout carried out as in (E) measuring the A$_7$-Broccoli-DFHBI-1T fluorescence generated over time.

(G) Inhibition of FTO in the m^{6}A$_7$-Broccoli assay. Titration the m^{6}A$_7$-Broccoli FTO reaction with four known inhibitors: rhein (red points), meclofenamic acid (Meclofen; blue points), FG4592 (purple points) and 2-4-pyridinedicarboxylate (2-4-pyr; orange points). This assay was carried out as in (E) with increasing inhibitor concentration. Data were normalized to the negative control (vehicle). n = 3. Error bars = SD.

fluorescent RNA-fluorophore complexes. We previously described Spinach, an RNA aptamer that binds and turns on the fluorescence of DFHBI, which is otherwise nonfluorescent (Paige et al., 2011, 2012). The crystal structure for Spinach revealed that the DFHBI ligand binds in a pocket formed between a G-quadruplex and a base triple with two flanking helices (Warner et al., 2014; Huang et al., 2014). Any disruption in the base triple or the G-quadruplex would be expected to cause a loss of fluorescence. Because of the diverse types of nucleotide interactions that are required for folding of the DFHBI-binding domain, we speculated that RNAs made with base modifications would disrupt these interactions and prevent fluorescent activation of DFHBI (Figure 1A). Particularly, base modifications in U or A may be expected to disrupt the base triple, while modifications of G would disrupt the G-quadruplex that is required for DFHBI binding. Furthermore, removal of the RNA modification via the appropriate RNA-modifying enzyme would then allow for proper RNA folding, DFHBI binding, and subsequent fluorescence.

For these experiments, we used Broccoli (Filonov et al., 2014), a brighter variant of Spinach. Broccoli exhibits high sequence identity in the core DFHBI-binding domain, and is therefore likely

to have a similar DFHBI-binding pocket to Spinach (Paige et al., 2011; Filonov et al., 2014) (Figure 1A). The previously described Broccoli was modified by adding a GC-rich stem to the 5′ and 3′ end resulting in a stabilized Broccoli containing nine adenosines (designated A_9-Broccoli; Figure S1C). In addition, we employed a modified DFHBI fluorophore, DFHBI-1T, which has fluorescence properties that better correlate with standard filter sets (Song et al., 2014).

To test whether some of the more prevalent naturally occurring RNA modifications affect the ability of Broccoli to bind and activate the fluorescence of DFHBI-1T, we transcribed A_9-Broccoli with specific modified nucleotide triphosphates. The fluorescence of modified A_9-Broccoli variants and A_9-Broccoli synthesized without modified nucleotides was compared. For nearly all forms of A_9-Broccoli synthesized with modified bases, the fluorescence was markedly reduced or abolished (Figure 1B). Thus, Broccoli is highly sensitive to diverse base modifications.

The markedly reduced fluorescence of m^6A-modified Broccoli is likely due to the loss of a key structural element, the U·A·U base triple that forms the upper surface of the DFHBI-binding pocket (Warner et al., 2014; Huang et al., 2014). The Spinach crystal structure reveals that the base triple is formed via Watson-Crick and Hoogstein base pairs between U·A·U, which involves both N^6-adenosine hydrogens (Figure 1C) (Warner et al., 2014; Huang et al., 2014). Thus, m^6A modification would prevent the hydrogen bond required for base triple formation (Figure 1C). Since this is essential for DFHBI binding, m^6A at this site would prohibit fluorescence.

Kinetic Analysis of FTO Reveals a Slow Turnover Rate

We reasoned that RNA-modifying enzymes could be assayed by their ability to restore the fluorescence of Broccoli containing base modifications. To test this idea, we focused on m^6A, a widespread mRNA modification in eukaryotes that can be demethylated by FTO in vitro (Jia et al., 2011) (Figure 1C). FTO has been implicated in neuronal function (Hess et al., 2013), responsiveness to cocaine, adipogenesis (Merkestein et al., 2015), and potentially other physiological processes. These discoveries implicate FTO as important regulators of physiological processes and a potential drug target. However, the mechanism by which FTO influences these diverse pathways remains to be elucidated, and the identification of potent and selective FTO inhibitors will be important for determining its function.

Although screens using FTO enzymatic activity have not been reported, several FTO inhibitors have been identified (Aik et al., 2013; Huang et al., 2015; Chen et al., 2012). These include meclofenamic acid (Huang et al., 2015) as well as rhein (Chen et al., 2012), which both inhibit FTO in cells. In addition, several nonspecific 2-oxoglutarate analogs were identified (Aik et al., 2013; Chen et al., 2012). The problem with these 2-oxoglutarate analogs is that they are expected to inhibit other 2-oxoglutarate-dependent enzymes. Another drawback of the previously described screens is that they were based on biochemical or computationally predicted FTO binding and not FTO enzymatic activity. As a result, only a fraction of FTO-binding compounds also show enzymatic inhibition (Rudolf et al., 2014). Thus, it is desirable to develop a screen that directly assays FTO enzymatic activity.

The major challenge in creating an enzymatic FTO HTS assay is the slow kinetics that has been reported for FTO when using m^6A-containing RNA as a substrate (k_{cat} = 0.30 min^{-1}) (Jia et al., 2011). In principle, the low FTO turnover rate could be overcome by simply adding more FTO in the assay. However, the enzyme concentration in an HTS assay should be below the substrate Michaelis-Menten constant (K_m) to ensure linear kinetics in the assay window (Acker and Auld, 2014; Brooks et al., 2004). This limits the concentrations of FTO and the substrate in the assay and hence the amount of fluorescence that can be generated.

We validated the FTO turnover rate on m^6A-containing RNA using a previously published HPLC-based assay (Kowalak et al., 1993; Jia et al., 2011). In this assay, m^6A-containing RNA is incubated with FTO and then degraded to nucleosides. The levels of A and m^6A can be quantified by their distinct migration as peaks on an HPLC chromatogram. The substrate in these assays was Broccoli that was transcribed with m^6A-triphosphate, so that the RNA contained only m^6A and no A (m^6A_9-Broccoli). In agreement with published FTO kinetic constants (k_{cat} = 0.30 min^{-1} and $K_{m,m^6A\text{-}RNA}$ = 0.60 μM) (Jia et al., 2011), we found the maximum turnover number (k_{cat}) to be 0.33 min^{-1} and $K_{m,m^6A\text{-}Broccoli}$ = 1.00 μM (Figure S1A). These measurements confirm that FTO exhibits slow turnover under the reaction conditions, and therefore FTO assays need to have high sensitivity and high signal output after a small number of turnovers.

Since phosphorylation can activate numerous proteins, we hypothesized that FTO activity could be improved by phosphomimetic mutations at phosphorylation sites that occur in eukaryotic cells. These phosphorylation events would not be present in the *Escherichia coli*-generated protein. Indeed, numerous phosphorylation events have been detected on FTO in proteome-wide screens for phosphorylation (Sharma et al., 2014; Olsen et al., 2010). To test this idea, we generated three phosphomimetic variants of human FTO predicted from published phosphoproteome datasets and tested them using the HPLC assay described above (Sharma et al., 2014; Olsen et al., 2010). However, none of these mutants (Y199E, S256D/S260D, and T4D/T6D) purified from *E. coli* showed a statistically significant increase in activity relative to the wild-type protein (Figure S1B). Based on this, we used wild-type recombinant FTO purified from *E. coli* and sought to optimize the assay sensitivity.

m^6A-Broccoli as a Fluorometric Substrate for FTO

Next we investigated whether m^6A_9-Broccoli could function as a fluorometric substrate for FTO. To test this, we used FTO to convert m^6A_9-Broccoli into a form that can bind and switch on the fluorescence of DFHBI-1T. m^6A_9-Broccoli was prepared by transcribing a Broccoli DNA template with m^6A-triphosphate, so that the RNA contained only m^6A and no A. We then treated m^6A_9-Broccoli with FTO using standard FTO assay conditions. We measured fluorescence following the addition of a Read buffer, which includes DFHBI-1T, KCl, and $MgCl_2$, to promote RNA folding (Figure 1D). This showed a moderate 2-fold increase in fluorescence, demonstrating that m^6A_9-Broccoli is a fluorometric substrate for FTO.

We next asked if we could increase the amount of fluorescence generated in this assay. Since FTO is a low-turnover-rate enzyme

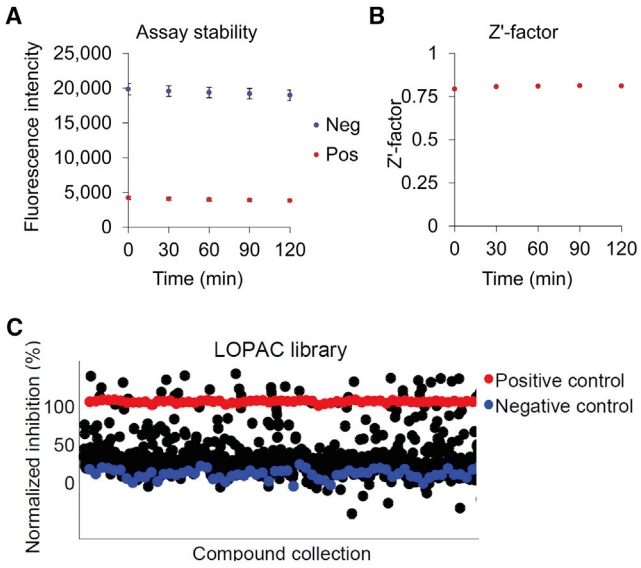

Figure 2. HTS of the LOPAC1280 Library Using the Broccoli FTO Assay

(A) Stability of the Broccoli HTS assay. The assay stability was measured for FTO-catalyzed m^6A_7-Broccoli demethylation in a standard HTS format using the fluorescence resulting from the A_7-Broccoli that is generated as a readout. The negative control (neg; blue points) was FTO-catalyzed m^6A_7-Broccoli demethylation and the positive control (pos; red points) was rhein at 90% inhibition. n = 192.

(B) Z′ factor of the Broccoli HTS assay. The Z′ factor was measured as described in (A) and calculated from Equation (1). n = 192. Error bars = SD.

(C) HTS of the LOPAC1280 library. m^6A_7-Broccoli FTO HTS of the LOPAC1280 library was carried out as described in (A) with test compounds at 10 μM. The negative control (blue points) and the positive control (red points) are as described in (A). The inhibition percent, compared with the negative control, was measured for each of the test compounds (black points) and normalized to the positive control. n = 16 for controls and n = 2 for test compounds.

on m^6A-containing RNA, we reasoned that a Broccoli that contains fewer than nine m^6A residues would require fewer turnovers to obtain fluorescent activation. To achieve this we created and tested the fluorescence of various reduced-adenosine Broccoli variants (Figure S1C). To identify adenosine residues that could be mutated without affecting Broccoli fluorescence, we performed adenosine mutagenesis and monitored the fluorescence of the reduced-adenosine Broccoli variants. This showed that substitution of the adenosine that is positioned immediately below the G-quadruplex in Broccoli was not tolerated (Figures S1C and S1D). In addition, most adenosine substitutions in the region above the base triple were also not tolerated, presumably due to destabilization of the base triple or the adjacent helix (Figures S1C and S1D; variants A_3-A_{6b}). However, in variant A_{5c}-Broccoli the helix complementarity was restored via U28C and U30C substitutions (Figure S1C). This resulted in partially rescued fluorescence compared with A_9-Broccoli (Figure S1D). Only the A_7-Broccoli variant with two adenosine substitutions at positions further removed from the base triple and G-quadruplex retained the ability to efficiently activate DFHBI-1T compared with A_9-Broccoli (Figures S1C and S1D). Thus, we selected A_7-Broccoli RNA for our FTO HTS assay.

Next we confirmed that methylated A_7-Broccoli (m^6A_7-Broccoli) is an improved fluorometric substrate for FTO. Indeed, FTO-treated m^6A_7-Broccoli yielded a 3-fold increase in fluorescence compared with the 2-fold fluorescence increase observed with m^6A_9-Broccoli (Figure 1D). A 3-fold increase in fluorescence is generally sufficient for reliable HTS (Palamakumbura and Trackman, 2002; Koresawa and Okabe, 2004). These data demonstrate that m^6A_7-Broccoli is an improved fluorometric substrate for FTO.

We were concerned that m^6A_7-Broccoli could potentially bind DFHBI-1T without turning on its fluorescence and thereby compete with A_7-Broccoli. To test this we titrated A_7-Broccoli in a solution containing m^6A_7-Broccoli at different DFHBI-1T concentrations. No interference by m^6A_7-Broccoli was observed, demonstrating that m^6A_7-Broccoli does not bind DFHBI-1T (Figure S1E).

We next asked if m^6A_7-Broccoli could be used to detect FTO activity in an enzyme- and time-dependent manner. Titration of FTO and a time course showed that the fluorescence was dependent on enzyme concentration (Figure 1E) and time (Figure 1F), with a linear increase in signal up to 50% conversion. These data are comparable to those observed using the previously published HPLC-based FTO assay (Jia et al., 2011) (Figure S2). These experiments confirm that the FTO assay using m^6A_7-Broccoli detects FTO activity in an enzyme- and time-dependent manner as expected for biochemical assays.

Lastly, we wanted to test the performance of this assay in dose-response studies of known FTO inhibitors. Thus, we titrated the m^6A_7-Broccoli FTO reaction with two known FTO inhibitors: rhein (Chen et al., 2012) and meclofenamic acid (Huang et al., 2015). This showed median inhibitory concentration (IC_{50}) values of 2.18 and 7.94 μM and inhibitor constant (K_i) values of 0.29 and 1.04 μM for rhein and meclofenamic acid, respectively (Figure 1G), which is comparable with the previously reported values (rhein, K_i = 1.8 μM, Chen et al., 2012; meclofenamic acid, IC_{50} = 16.7 μM, Huang et al., 2015). These data demonstrate that this assay allows measurement of IC_{50} curves of FTO inhibitors.

Z′ Factor of the Broccoli-Based FTO HTS Assay

We next asked if the FTO assay using m^6A_7-Broccoli is suitable for HTS. The Z′ factor (Zhang et al., 1999) is the most commonly used metric to define HTS assay quality as it allows determination of statistically significant inhibition or activation in an assay (Equation 1). We measured the Z′ factor in an HTS format using FTO demethylation of m^6A_7-Broccoli at 10% conversion in a full 384-well plate using automatic dispensing. Thus, we incubated m^6A_7-Broccoli with FTO and monitored fluorescence following incubation with Read buffer, which promotes RNA folding and DFHBI-1T activation. The FTO inhibitor, rhein, was used as positive control at 90% inhibition and vehicle (DMSO) was used as the negative control. This showed a robust and stable fluorescent signal with a $Z' \geq 0.8$ at low substrate conversion over 2 hr (Figure 2). This demonstrates that m^6A_7-Broccoli provides a robust fluorometric HTS assay for FTO.

HTS of the LOPAC1280 Library with the Broccoli-Based FTO Assay

We next sought to optimize the FTO HTS screen to reduce the likelihood of obtaining nonspecific inhibitors. Many of the

previously described FTO inhibitors function as nonspecific competitors of 2-oxoglutarate, and can inhibit other 2-oxoglutarate-dependent enzymes (Aik et al., 2013; Chen et al., 2012). We tested whether the use of high concentrations of 2-oxoglutarate would reduce the ability of the 2-oxoglutarate analogs FG4592 and 2-4-pyridinedicarboxylate (Aik et al., 2013) to inhibit FTO. In the FTO assay with high 2-oxoglutarate concentrations, these 2-oxoglutarate analogs showed no inhibitory effect on FTO (Figure 1G). This indicates that inclusion of increased 2-oxoglutarate levels in the Broccoli FTO assay reduces interference from undesirable 2-oxoglutarate competitive analogs during HTS.

Next we screened the LOPAC1280 compound collection for FTO inhibitors. This library consists of 1,280 structurally diverse, high-purity, small organic compounds (Lazo et al., 2007). The compounds include those with well-documented pharmacological activities, as well as compounds with known activities against orphan receptors (Lazo et al., 2007). This makes the LOPAC1280 library useful for HTS assay validation (Rickardson et al., 2006).

The Broccoli-based FTO HTS with the LOPAC1280 library was carried out using the HTS format and the controls described above. Compounds were tested at 10 μM final concentration in two replicates. Under these conditions the assay showed a Z' factor = 0.7 and a 3-fold increase in the mean fluorescence intensity of positive controls compared with the negative control signal (Figure 2C). These data show that the positive and the negative controls are well resolved in the assay window and that several compounds exhibit FTO inhibition comparable to the positive control. Hits were identified with the cut-off of 75%–115% inhibition normalized to the positive control and $Z' > 0.5$. This identified 25 inhibitors (**1**–**25**) corresponding to a hit rate of 2.0%, which falls within an expected hit rate of 1%–5% of this library (Figures 3, S3, and S4). Thus, HTS using the Broccoli assay allows identification of FTO inhibitors.

A_7-Broccoli-Based Counter Screening to Exclude False Positives

Next we sought to exclude nonspecific inhibitors. Compounds that directly bind Broccoli and displace the fluorophore from the RNA-binding pocket could yield false positives. To exclude these nonspecific compounds we performed a counter screen in which we tested whether the compounds could prevent A_7-Broccoli from binding DFHBI-1T. To do this we measured IC_{50} and calculated the K_i of the 25 identified hits both for FTO using m^6A_7-Broccoli and for Broccoli-DFHBI-1T complex formation using A_7-Broccoli. This was performed using the Broccoli HTS assay format and controls described above (Table 1 and Figure S5) (Neubig et al., 2003). Of the 25 hits, **1**–**19** were designated as specific since they displayed an FTO $K_i < 1.5$ μM and an $IC_{50} > 20$ μM for A_7-Broccoli-DFHBI-1T complex formation (Table 1). This demonstrates that the majority of hits from the Broccoli HTS assay were specific FTO inhibitors compared with the nonspecific inhibitors of Broccoli itself.

Structural Characterization of the Identified Inhibitors

Notably, **1**–**12** do not exhibit structural similarity to any of the previously described FTO inhibitors (Aik et al., 2013; Huang et al., 2015; Chen et al., 2012) (Figure 3). Interestingly, two new distinct classes of structural motifs were identified among these 12 compounds: **1**–**3** belong to the amiloride class, whereas **4**–**7** are metizolines.

We hypothesized that these two compound groups represent new overall classes of FTO inhibitors. To validate this idea, we searched for structures with >70% similarity to **3** and **5** in the LOPAC1280 library and compared their normalized percent inhibition in the m^6A_7-Broccoli FTO HTS dataset. This identified an additional four amiloride derivatives (**26**–**29**) and three metizoline derivatives (**30**–**32**), which all showed significant normalized inhibition (23%–122%; Figures S3A and S3B). These inhibitors were not identified in the initial analysis, because these compounds show inhibition above or below the applied cut-off of 75%–115% normalized inhibition (Figure S3B). This identifies amiloride and metizoline as pharmacophores for FTO inhibitors.

In addition to these novel inhibitors, we also observed compounds similar to rhein and meclofenamic acid (**13**–**19**; Figure 3). Thus, the FTO screen revealed both novel and previously known structural classes of FTO inhibitors.

Importantly, unlike previous FTO screens, none of the inhibitors identified here show similarity to 2-oxoglutarate (Aik et al., 2013; Chen et al., 2012) (Figure 3). This is consistent with the idea that inclusion of increased concentrations of 2-oxoglutarate in the assay excludes competitive inhibitors of this cofactor.

Some of the FTO inhibitors were polyphenols. Polyphenols, such as catechols, often appear as frequent hitters in many biochemical HTS assays (Baell and Holloway, 2010). However, all the identified polyphenol hit compounds in this assay are rhein analogs (**13**–**16**). Rhein is a previously reported FTO inhibitor with demonstrated in vivo efficacy. This suggests that the polyphenols identified in this study are likely to inhibit FTO via specific mechanisms.

Nonspecific Inhibitors Are Planar Molecules or Nucleotide Structural Analogs

We next examined the nonspecific inhibitors that blocked DFHBI-1T binding to Broccoli. Evaluation of their structural motifs (Table 1, A_7-Broccoli $IC_{50} < 20$ μM) could allow identification and exclusion of these compounds from hit collections. It is noticeable that four (**20**–**23**) of six false positives have structures that appear to be planar, similar to DFHBI-1T (Figure S4). This may be an indication that these molecules may exhibit their interference by competing with DFHBI-1T binding. The rest (**24**–**25**) have structure similarity to the purine ring in adenosine and guanosine in Broccoli, and thus may bind to Broccoli or interfere with its folding. It is notable that **20**–**22** and **24**–**25** all show significantly stronger inhibition in the FTO assay compared with the A_7-Broccoli counter screen (Table 1). This indicates that these compounds may potentially be FTO inhibitors in addition to exhibiting nonspecific interference. The fact that all the nonspecific inhibitors resemble DFHBI-1T or purine in RNA enables identification and hence exclusion of library members that may be false positives.

Inhibitor Potency Is in the Nanomolar Range

Next we sought to evaluate the potency of the identified inhibitors compared with previously reported FTO inhibitors. Three of the FTO inhibitors with novel structures (**1**, **4**, and **8**) show

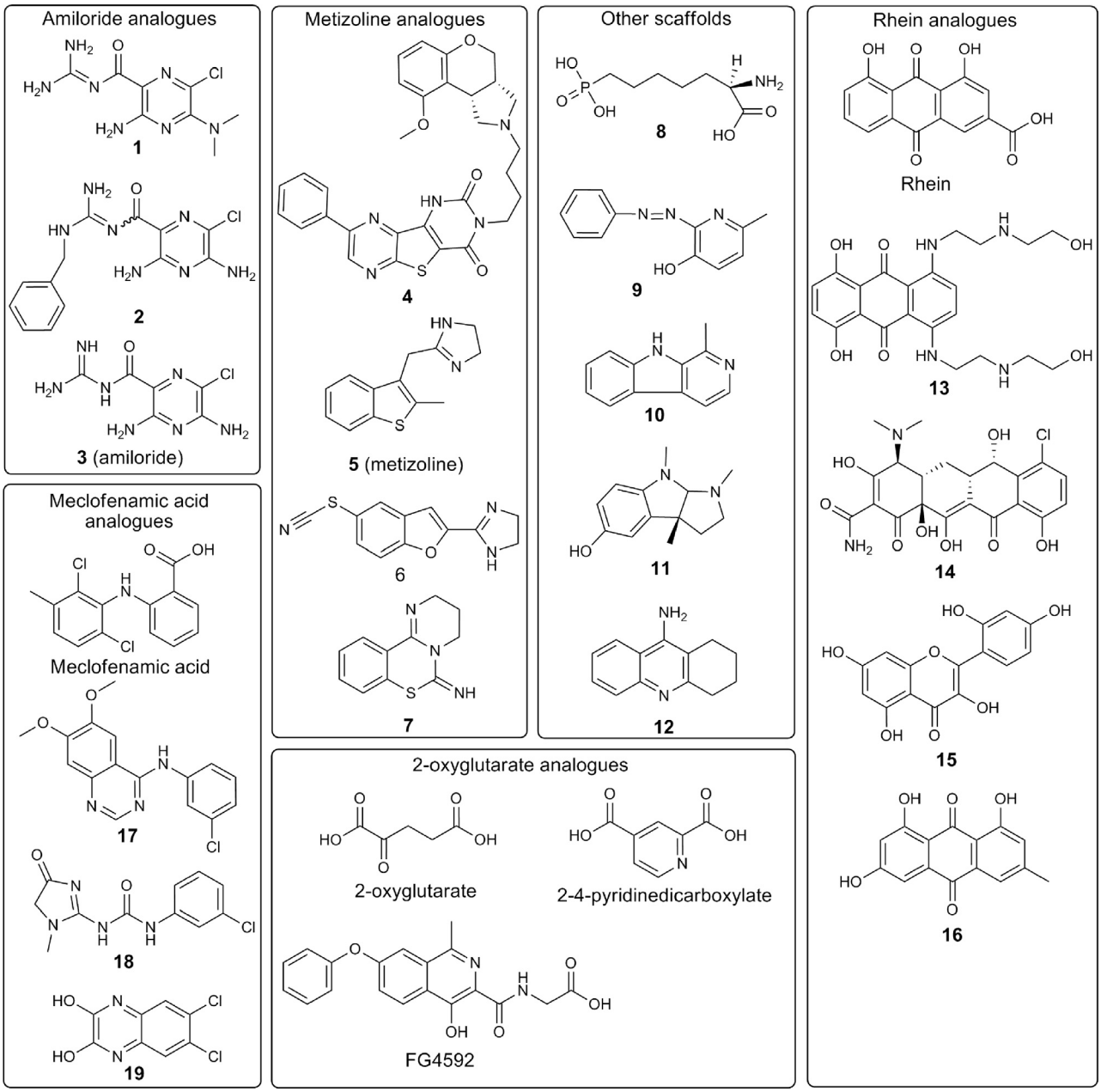

Figure 3. Structures of FTO Inhibitors Identified from LOPAC1280

Screen hits from m^6A_7-Broccoli FTO HTS were identified using a cut-off of 75%–115% normalized inhibition and $Z' > 0.5$.

potent inhibition in the nanomolar range (K_i = 40.4, 57.9, and 99.4 nM, respectively), which is more potent than any other published FTO inhibitors (Aik et al., 2013; Huang et al., 2015; Chen et al., 2012) (Figure S3 and Table 1). Together, these data demonstrate that the Broccoli-based HTS assay is a powerful tool for identification of potent inhibitors of RNA-modifying enzymes.

Validation of Inhibition in Secondary Format

Next we sought to further validate the identified hits in a secondary assay. Eight of the commercially available hit compounds (**1**, **5**, **8**, **10**, **11**, **13**, **14**, and **15**) were tested using the HPLC method described earlier (Figures S6A–S6D). In addition, the previously reported FTO inhibitor, rhein (Chen et al., 2012), was included as a positive control. The K_i values calculated from the IC_{50} curves for all the nine compounds in the HPLC assay were comparable to those obtained via the fluorescent readout in the Broccoli HTS assay format (Figures S6A–S6D). These experiments confirm that these compounds inhibit FTO and demonstrates that the K_i values obtained by the fluorometric FTO assay correlate with those obtained by the HPLC assay.

Table 1. List of FTO Inhibitors Identified from LOPAC Screen and their Measured IC_{50} and Pharmacokinetic Properties

Compound Number	IC_{50} (μM) on FTO	K_i (nM) on FTO	IC_{50} (μM) on Broccoli	log P	Lipinski Violations	Cytotoxicity NPCD (%)	Structural Analogs
1	0.34	40	>20	0.05	0	−3.18	
2	2.79	328	>20	1.11	0	8.97	amiloride
3	4.74	558	>20	−0.50	0	4.26	
4	0.49	58	>20	4.29	1	70.10	metizoline
5	1.37	161	>20	2.73	0	9.03	
6	1.62	191	>20	1.60	0	21.54	
7	2.18	256	>20	2.10	0	2.10	
8	0.85	99	>20	−2.35	0	8.39	
9	1.14	134	>20	3.58	0	24.37	
10	1.23	145	>20	2.00	0	−0.79	other
11	1.27	149	>20	2.43	0	19.53	
12	1.71	201	>20	2.63	0	4.05	
13	1.20	141	>20	1.19	1	78.93	rhein
14	1.39	164	>20	−3.21	1	13.88	
15	2.58	304	>20	2.16	0	6.32	
16	4.53	533	>20	3.82	0	14.70	
17	3.00	353	>20	3.75	0	35.77	meclofenamic acid
	3.31	389	>20	0.98	0	−9.08	
19	4.97	585	>20	3.09	0	7.95	
20	0.71	83	13.60	3.34	0	7.75	planar
21	3.13	368	6.60	−3.59	0	73.40	
22	5.19	611	10.10	1.98	0	21.75	
23	8.48	998	7.00	1.33	0	4.01	
24	1.34	158	3.47	2.94	0	27.20	purine
25	2.57	302	14.50	1.71	0	1.34	

LogP, Lipinski violation, and cytotoxicity (normalized percent cell death [NPCD]) data were available from the High-Throughput Screening Resource Center at Rockefeller University through the Collaborative Drug Discovery software. NPCD was measured using the Cell Titer Glo Assay (Promega) at 10 μM compound in SK-N-SH, MRC5, and HepG2 cells. K_i was calculated as $K_i = IC_{50}/(1 + [substrate]/K_m)$. Previously reported drug targets for each compound are listed in Table S1.

Identification of Inhibitors Selective for FTO over ALKBH5

We next asked if the inhibitors identified here are selective for FTO over another 2-oxoglutarate-dependent m^6A-demethylase, ALKBH5. The commercially available inhibitors with high potency (**1** and **8**) and superior pharmacokinetic properties (**1**, **10**, and **11**), as well as the least cytotoxic rhein analog (**15**), were tested. In addition, the nonselective inhibitor, rhein (Chen et al., 2012), and the FTO-selective inhibitor, meclofenamic acid (Huang et al., 2015), were included as controls. The IC_{50} curves were measured using the fluorescent readout in the Broccoli HTS assay as described earlier (Figure 4). Compounds **8**, **11**, and meclofenamic acid were FTO selective and did not inhibit ALKBH5 (IC_{50} > 20 μM), whereas **1** and **10** showed efficient ALKBH5 inhibition (K_i < 300 nM). Rhein and its analog (**15**) both showed weak ALKBH5 inhibition ($K_i \sim 1$ μM), which is consistent with previous reports (Huang et al., 2015; Chen et al., 2012). Noticeably, there are no obvious structural features that distinguish the FTO-selective inhibitors (**8**, **11**, and meclofenamic acid) from inhibitors that also inhibit ALKBH5 (**1**, **10**, **15**, and rhein). These data demonstrate that the Broccoli HTS assay enables identification of FTO-selective inhibitors as well as inhibitors that target both ALKBH5 and FTO.

Next we asked if the identified compounds are competitive inhibitors. To determine the mode of inhibition for the best inhibitors we generated Lineweaver-Burk plots (Lineweaver and Burk, 1934) to assay for RNA substrate competition. FTO-catalyzed demethylation was measured with increasing amounts of m^6A_7-Broccoli in the presence of inhibitors. The commercially available inhibitors with high potency (**1**) and superior pharmacokinetic properties (**1**, **10**, and **11**), as well as the least cytotoxic rhein analog (**15**) were tested. This showed that **10**, **11**, and **15** are competitive inhibitors, whereas **1** shows mixed inhibition (Figure S6E). These data demonstrate that the Broccoli HTS assay enables identification of both competitive and mixed inhibitors.

Drug Likeness and Cytotoxicity Evaluation of the Identified Inhibitors

FTO inhibitors may be useful for studying FTO functions in live animals or in cells. To determine if the inhibitors identified here could be used for this purpose, we examined their pharmacokinetic properties and cytotoxicity (Table 1). Cytotoxicity,

A

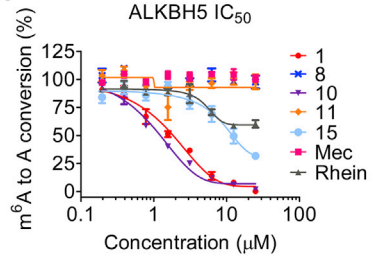

B

#	ALKBH5 IC_{50} (μM)	ALKBH5 K_i (μM)
1	1.98	0.23
8	> 20	-
10	1.24	0.15
11	> 20	-
15	7.13	0.84
Mec	> 20	-
Rhein	9.96	1.17

Figure 4. Selectivity of FTO Inhibitors toward ALKBH5

(A) IC_{50} curves of AKLBH5 inhibition in the m^6A_7-Broccoli-based assay. ALKBH5-mediated demethylation of m^6A_7-Broccoli was assayed with increasing amounts of inhibitors. The extent of ALKBH5-catalyzed m^6A_7-Broccoli demethylation was measured using the fluorescence resulting from the generated A_7-Broccoli. Data were normalized to the positive control (vehicle).

(B) IC_{50} values of AHKBH5 inhibition in the m^6A_7-Broccoli-based assay. The ALKBH5 IC_{50} values were measured at 50% m^6A to a conversion from IC_{50} curves in (A). K_i was calculated as $K_i = IC_{50}/(1 + [substrate]/K_m)$. n = 3. Error bars = SD.

partition coefficient (logP), and Lipinski violation data were available from the High-Throughput Screening Resource Center at Rockefeller University through the Collaborative Drug Discovery software (Hohman et al., 2009). Four compounds (**1**, **5**, **10**, and **11**) show superior pharmacokinetic properties based on the following constraints: FTO K_i < 150 nM; logP between −0.5 and 5; no Lipinski violations; and cytotoxicity measured as normalized percent cell death <20%. Interestingly, all four compounds belong to the new structural motif categories.

Inhibition of FTO Demethylation of Target Transcripts in Cells

Next we sought to determine if the FTO inhibitors affect methylation levels of FTO-regulated transcripts in cells. FTO is relatively selective in that most m^6A-containing mRNAs are not demethylated in vivo (Hess et al., 2013). The target transcripts were selected from a previously published list of FTO-regulated transcripts with the following constraints: (1) FTO regulation of methylation levels in transcripts based on analysis of brain mRNA from FTO knock-out mice (Hess et al., 2013) and (2) validated methylation sites in the 5′UTR of the same mRNA in HEK293 cells (Linder et al., 2015). Based on these criteria, we selected bone morphogenetic protein 6 (*BMP6*) and ubiquitin C (*UBC*) for validation in cells according to previously published procedures (Meyer et al., 2012). We used an antibody selective for 6-methyladenine in immunoprecipitation assays to isolate methylated mRNAs from total RNA from HEK293 cells treated with vehicle or the FTO inhibitor for 48 hr. *BMP6* and *UBC* transcript levels were quantified in the immunoprecipitation fractions by reverse transcription qPCR.

The efficacy of the commercially available inhibitors with high potency (**1** and **8**) and superior pharmacokinetic properties (**1**, **10**, and **11**), as well as the least cytotoxic rhein analog (**15**), were tested in cells. All transcripts were normalized to the amount glyceraldehyde-3-phosphate dehydrogenase (*GAPDH*) mRNA in the unbound fraction within each sample. *GAPDH* was chosen because it is an abundant transcript which does not have FTO-regulated m^6A peaks (Hess et al., 2013). Compared with the amount of RNA from vehicle-treated cells the levels of *BMP6* and *UBC* transcripts were substantially decreased in the **8**-, **10**-, and **15**-treated unbound 6-methyladenine-immunoprecipitation fractions (Figure 5). These data indicate that **8**, **10**, and **15** can inhibit FTO and reduce FTO-mediated demethylation activity in cells.

DISCUSSION

The fluorometric Broccoli substrate allows for a simple mix-and-measure assay format. This direct readout format circumvents the disadvantages associated with current HPLC/MS-based RNA-modifying enzyme assays such as: the need for fluorescently or radioactively labeled substrates; the potential for test compound interference with secondary coupling enzyme reactions; and the need for separation steps prior to HPLC or MS analysis.

The Broccoli-based fluorometric substrates, and their cognate fluorophores, have properties that make them well-suited for HTS applications. The fluorescent signal is stable over time and in a variety of buffers. They also bind a variety of fluorophores with adjustable spectral properties in a plug-and-play fashion (Song et al., 2014). In addition, RNA modifications can easily be incorporated into Broccoli by in vitro transcription, and most modified Broccoli variants are nonfluorescent. These unique properties enable flexibility in the Broccoli HTS assay as they allow tailoring of the spectral readout and the RNA modification to suit the target of choice.

As an example, we applied the Broccoli HTS assay to one of the most prominent RNA-modifying enzymes, FTO. We demonstrated that upon FTO-catalyzed demethylation of m^6A_7-Broccoli, the RNA regained fluorescence, which could be detected in an HTS format in an enzyme-concentration- and time-dependent manner. This was followed by an HTS with the LOPAC-1280 compound library. The Broccoli FTO HTS assay showed high HTS performance metrics with a Z′ factor >0.7 and hit rate of 2.0%.

The FTO inhibitors identified here are more potent than previously described FTO inhibitors, with three of these inhibitors (**1**, **4**, and **8**) exhibiting K_i values in the nanomolar range (40.4, 57.9, and 99.4 nM, respectively).

Importantly, the majority of the FTO inhibitors (12 compounds) do not exhibit significant structural similarity to any of the reported FTO inhibitors. Interestingly, two new distinct classes of structural motifs were identified: seven amiloride analogs inhibitors (**1**–**3**, **26**–**29**) and seven metizoline analogs inhibitors (**4**–**7**, **30**–**32**), which all showed significant inhibition. Together, these data demonstrate that the Broccoli-based HTS assay is a powerful tool for identification of potent and selective RNA-modifying enzyme inhibitors including new structural motifs.

Notably, only a few of the identified inhibitors showed nonspecific interactions by inhibiting the Broccoli-DFHBI-1T complex

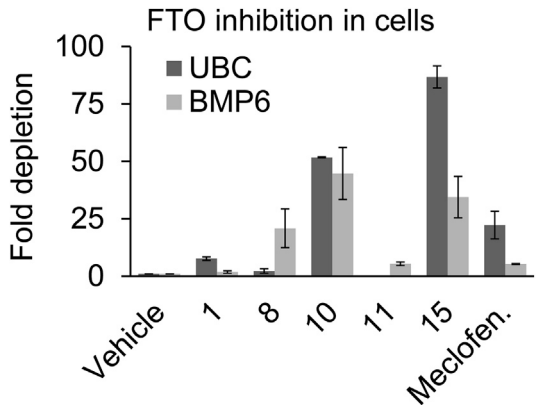

Figure 5. Inhibition of FTO-Mediated Demethylation of Target Transcripts in Cells

The effect of FTO inhibitors on demethylation of an FTO-regulated transcript was determined in HEK293T cells. Cells were treated for 48 hr with the compound at 30 μM, which is >100-fold than the measured K_i for the tested compounds. Afterwards, the total RNA was isolated and 6-methyladenine containing mRNAs were isolated by immunoprecipitation using a 6-methyladenine-specific antibody. Unbound RNAs were isolated, and the abundance of the target *BMP6* and *UBC* transcripts was measured by reverse transcription qPCR. All samples were normalized the amount of *GAPDH* mRNA in the unbound fraction within each sample. n = 2. Error bars = SD.

rather than FTO. These nonspecific inhibitors have planar structures similar to DFHBI-1T (**20**–**23**), or to the purine ring in adenosine and guanosine in RNA (**24**–**25**). To reduce the likelihood of identifying false positives in an initial screen, compounds with these structures can easily be excluded from hit collections prior to hit validation in future screens.

Several of the FTO inhibitors identified here show selectivity for FTO over ALKBH5, another m^6A-demethylating enzyme. Nonselective inhibition can arise with inhibitors that target the 2-oxoglutarate-binding site or other conserved domains found in this enzyme family. Indeed, these types of inhibitors were identified in previous screens (Aik et al., 2013; Huang et al., 2015; Chen et al., 2012). The use of elevated 2-oxoglutarate concentrations in the assay likely accounts for the reduced number of inhibitors that exhibit direct similarity to 2-oxoglutarate.

Furthermore, we showed that Broccoli synthesized with most other modified nucleotides also blocked Broccoli fluorescence. Conceivably Broccoli synthesized with these other modifications could function as fluorometric substrates in HTS of the RNA-modifying enzymes that regulate the respective RNA modifications (Table S2). Interestingly, one modification (5-methylcytidine; m^5C), significantly increased Broccoli fluorescence. m^5C modifications are known to increase duplex stability due to enhanced base stacking (Luyten and Herdewijn, 1998). Broccoli contains eight base-paired cytosine residues in the helical regions, and the subsequent helical stabilization may explain the increased fluorescence observed for m^5C-Broccoli. Analogous to the RNA modifications that decrease fluorescence, modifications that increase fluorescence could be measured in enzyme assays where the modification is added by the respective RNA-modifying enzyme.

SIGNIFICANCE

RNA-modifying enzymes are important regulators of physiological processes, but are difficult to assay due to the absence of fluorometric substrates. As a result, these enzymes are assayed in complex assays requiring multiple enzymatic processing steps following by HPLC- and MS-based detection of the modified nucleotide products. Here we describe a fluorometric substrate for FTO based on the Broccoli aptamer. Upon demethylation by FTO or ALKBH5, the methylated Broccoli is switched to a demethylated form, allowing it to bind and activate the fluorescence of DFHBI-1T. Furthermore, the FTO assay using the methylated Broccoli shows a high Z′ factor (>0.8) suitable for HTS. Using this assay, we identify novel FTO inhibitors that show higher potency than previously described. Several of these new structures showed selectivity for FTO over the related demethylase, ALKBH5, and influenced methylation of endogenous FTO target mRNAs in cells. We generated modified Broccoli-based fluorometric substrates for a diverse range of RNA-modifying enzymes, which show that this approach is generally applicable for HTS of RNA-modifying enzymes.

EXPERIMENTAL PROCEDURES

Reagents and Equipment

Unless otherwise stated, all reagents were purchased from Sigma-Aldrich. DFHBI-1T was from Lucerna Technologies (New York, NY) or prepared as described previously (Paige et al., 2011). Commercially available reagents were used without further purification. All HTS assays were performed at the High-Throughput Screening Resource Center at Rockefeller University. Fluorescence intensity was measured with a BioTek Synergy NEO plate reader equipped with fluorescein isothiocyanates (FITC) filters. Unless otherwise stated all assays were performed in a 384-flat-bottom-well black assay plate (Corning, 3573), which was sealed with an aluminum cover (Corning, 6570) during incubation and mixing. Automatic liquid dispensing was performed with a Thermo Multi-Drop Combi.

Broccoli-Based FTO and ALKBH5 Demethylation Assays

FTO demethylation reactions were performed by adding m^6A_7-Broccoli RNA (7.5 μM) or A_7-Broccoli RNA (7.5 μM) to a standard FTO assay buffer (FTO 1× buffer: 50 mM NaHEPES [pH 6], 300 μM 2-oxoglutarate, 300 μM $(NH_4)_2Fe(SO_4)_2 \cdot 6H_2O$, and 2 mM ascorbic acid in RNase-free H_2O) on ice, followed by addition of FTO (0.250–3 μM) from stock (10 μM) in PPB C (above) in a 40-μl volume. The FTO assay components were mixed on ice immediately before incubation. The FTO assay mixture was added to a standard 384-flat-bottom-well black assay plate (40 μl in each well). The plates were sealed with a plastic cover, spun at 1,000 × *g* for 30 s, shaken for 3 min, and incubated for at 37°C for 2 hr (unless otherwise stated).

During enzyme inhibition studies, inhibitors (rhein [Selleck Chemicals], meclofenamic acid, FG4592, 2-4-pyridinedicarboxylate), or vehicle (DMSO) were added to the wells prior to FTO (250 nM) or ALKBH5 (250 nM).

For fluorescence experiments FTO Read buffer 5× (250 mM NaHEPES [pH 9], 1,000 mM KCl, 40 mM $MgCl_2$, 2.2 μM DFHBI-1T in RNase-free H_2O) was added to each well (10 μl; 50 μl final volume). The plates were sealed with a plastic cover, spun at 1,000 × *g* for 30 s, shaken for 3 min, and incubated for 2 hr at room temperature and 16 hr at 4°C to allow the A_7-Broccoli RNA to fold and bind DFHBI-1T. The fluorescence intensity was measured with a BioTek Synergy NEO plate reader with FITC filters. Automatic liquid dispensing was performed with a Thermo Multi-Drop Combi.

Measurement of Z′ Factor of the Broccoli-Based FTO HTS Assay

Z′ factor measurements were carried out as described above with FTO (250 nM) as well as vehicle (0.2% DMSO) or rhein (30 μM in 0.2% DMSO)

added to the FTO assay buffer prior to dispensing (40 μl) in 192 wells for each. The Z′ factor was calculated using the average fluorescence of rhein wells as the positive control (pos) and the average fluorescence of vehicle (DMSO) wells as the negative control (neg) using Equation (1).

$$Z' = 1 - 3 \times [\sigma_{neg} + \sigma_{pos}]/([\mu_{neg} - \mu_{pos}]. \quad (1)$$

HTS of LOPAC1280 Library and Hit IC_{50} Measurement with the Broccoli FTO Assay

HTS of the LOPAC1280 compound collection (Sigma-Aldrich) with the Broccoli FTO assay was carried out in a standard 384-flat-bottom-well black assay plate (50 μl final volume per well). Compounds (5 mM stock in DMSO) were deposited at 80 nl per well (final 10 μM in 0.2% DMSO) into plates containing NaHEPES (pH 6) (10 μl, 50 mM) per well. Negative and positive control wells (16 of each per plate) were set up analogously with vehicle (final 0.2% DMSO) and rhein (final 30 μM in 0.2% DMSO), respectively.

FTO Assay Master Mix 1.33× (50 mM NaHEPES [pH 6], 400 μM 2-oxoglutarate, 400 μM $(NH_4)_2Fe(SO_4)_2 \cdot 6H_2O$, and 2.67 mM ascorbic acid , 10 μM m^6A_7-Broccoli, hFTO in 333 nM PPB C in RNase-free H_2O) was mixed on ice immediately before dispensing (30 μl per well; 40 μl total volume). The plates were sealed with an aluminum cover (Corning, 6570), spun at 1,000 × *g* for 30 s, shaken for 2 min, and incubated at 37°C for 2 hr.

FTO Read buffer 5× was dispensed (10 μl per well; 50 μl total volume). The plates were sealed with an aluminum cover, spun at 1,000 × *g* for 30 s, shaken for 2 min, and incubated for 2 hr at room temperature and 16 hr at 4°C to allow the A_7-Broccoli RNA to fold and bind DFHBI-1T. The fluorescence intensity was measured with a BioTek Synergy NEO plate reader with an FITC filter. Automatic liquid dispensing was performed with a Thermo Multi-Drop Combi.

IC_{50} curves of **1**–**25** inhibition of FTO, as well as meclofenamic acid, **1**, **8**, **10**, **11**, and **15** inhibition of ALKBH5, were carried out as described for the HTS of the LOPAC1280 library with ten serial dilutions of each compound starting at 20 μM.

Replicates of test compounds were carried out on two different days in random wells. The raw data transferred to CDD Vault Collaborative Drug Discovery software (Hohman et al., 2009), where correlation of replicates and data analysis including normalization and IC_{50} curve fitting was performed.

SUPPLEMENTAL INFORMATION

Supplemental Information includes Supplemental Experimental Procedures, six figures, and two tables and can be found with this article online at http://dx.doi.org/10.1016/j.chembiol.2015.11.018.

AUTHOR CONTRIBUTIONS

N.S. and S.R.J. conceived and designed the experiments, N.S. performed all experiments and analyzed data, and N.S. and S.R.J. wrote the manuscript.

ACKNOWLEDGMENTS

We thank Wenjiao Song (Weill Cornell Medical College) for synthesis of DFHBI-1T, Alexander Serganov (New York University) for FTO plasmid, and Fraser Glickman and Jeanne Chiaravalli at The Rockefeller University High Throughput and Spectroscopy Resource Center for providing assay guidance, instrumentation and infrastructure to conduct this study. This work was supported by NIH R01 DA037150 and R01 NS064516 to S.R.J.

Received: September 4, 2015
Revised: November 10, 2015
Accepted: November 20, 2015
Published: February 11, 2016

REFERENCES

Acker, M.G., and Auld, D.S. (2014). Considerations for the design and reporting of enzyme assays in high-throughput screening applications. Perspect. Sci. *1*, 56–73.

Aik, W., Demetriades, M., Hamdan, M.K., Bagg, E.A., Yeoh, K.K., Lejeune, C., Zhang, Z., McDonough, M.A., and Schofield, C.J. (2013). Structural basis for inhibition of the fat mass and obesity associated protein (FTO). J. Med. Chem. *56*, 3680–3688.

Baell, J.B., and Holloway, G.A. (2010). New substructure filters for removal of pan assay interference compounds (PAINS) from screening libraries and for their exclusion in bioassays. J. Med. Chem. *53*, 2719–2740.

Barwick, V.J. (1999). Sources of uncertainty in gas chromatography and high-performance liquid chromatography. J.Chromatogr. A *849*, 13–33.

Brooks, H.B., Geeganage, S., Kahl, S.D., Montrose, C., Sittampalam, S., Smith, M.C., and Weidner, J.R. (2004). Basics of enzymatic assays for HTS. In Assay Guidance Manual [Internet], G.S. Sittampalam, N.P. Coussens, H. Nelson, M. Arkin, D. Auld, C. Austin, B. Bejcek, M. Glicksman, J. Inglese, and P.W. Iversen, et al., eds. (Eli Lilly and the National Center for Advancing Translational Sciences).

Chen, B., Ye, F., Yu, L., Jia, G., Huang, X., Zhang, X., Peng, S., Chen, K., Wang, M., Gong, S., et al. (2012). Development of cell-active N6-methyladenosine RNA demethylase FTO inhibitor. J. Am. Chem. Soc. *134*, 17963–17971.

Crespi, C.L., Miller, V.P., and Stresser, D.M. (2002). Design and application of fluorometric assays for human cytochrome P450 inhibition. Methods Enzymol. *357*, 276–284.

Filonov, G.S., Moon, J.D., Svensen, N., and Jaffrey, S.R. (2014). Broccoli: rapid selection of an RNA mimic of green fluorescent protein by fluorescence-based selection and directed evolution. J. Am. Chem. Soc. *136*, 16299–16308.

Hess, M.E., Hess, S., Meyer, K.D., Verhagen, L.A., Koch, L., Brönneke, H.S., Dietrich, M.O., Jordan, S.D., Saletore, Y., Elemento, O., et al. (2013). The fat mass and obesity associated gene (Fto) regulates activity of the dopaminergic midbrain circuitry. Nat. Neurosci. *16*, 1042–1048.

Hohman, M., Gregory, K., Chibale, K., Smith, P.J., Ekins, S., and Bunin, B. (2009). Novel web-based tools combining chemistry informatics, biology and social networks for drug discovery. Drug Discov. Today *14*, 261–270.

Huang, Y., Suslov, N.B., Li, N.S., Shelke, S.A., Evans, M.E., Koldobskaya, Y., Rice, P.A., and Piccirilli, J.A. (2014). A G-quadruplex–containing RNA activates fluorescence in a GFP-like fluorophore. Nat. Chem. Biol. *43*, 373–384.

Huang, Y., Yan, J., Li, Q., Li, J., Gong, S., Zhou, H., Gan, J., Jiang, H., Jia, G.F., Luo, C., et al. (2015). Meclofenamic acid selectively inhibits FTO demethylation of m6A over ALKBH5. Nucleic Acids Res. *43*, 373–384.

Jaffrey, S.R. (2014). An expanding universe of mRNA modifications. Nat. Struct. Mol. Biol. *21*, 945–946.

Jia, G., Fu, Y., Zhao, X., Dai, Q., Zheng, G., Yang, Y., Yi, C., Lindahl, T., Pan, T., Yang, Y.G., et al. (2011). N6-methyladenosine in nuclear RNA is a major substrate of the obesity-associated FTO. Nat. Chem. Biol. *7*, 885–887.

Koresawa, M., and Okabe, T. (2004). High-throughput screening with quantitation of ATP concentration: a universal non-radioactive, homogenous assay for protein kinase. Assay Drug Dev. Technol. *2*, 153–160.

Kowalak, J.A., Pomerantz, S.C., Crain, P.F., and McCloskey, J.A. (1993). A novel method for the determination of post-transcriptional modification in RNA by mass spectrometry. Nucleic Acids Res. *25*, 4577–4585.

Lazo, J.S., Brady, L.S., and Dingledine, R. (2007). Building a pharmacological lexicon: small molecule discovery in academia. Mol. Pharmacol. *72*, 1–7.

Li, S., and Mason, C.E. (2014). The pivotal regulatory landscape of RNA modifications. Annu. Rev. Genomics Hum. Genet. *15*, 127–150.

Limbach, P.A., Crain, P.F., and McCloskey, J.A. (1994). Summary: the modified nucleosides of RNA. Nucleic Acids Res. *22*, 2183–2196.

Linder, B., Grozhik, A.V., Olarerin-George, A.O., Meydan, C., Mason, C.E., and Jaffrey, S.R. (2015). Single-nucleotide-resolution mapping of m6A and m6Am throughout the transcriptome. Nat. Methods *12*, 767–772.

Lineweaver, H., and Burk, D. (1934). The determination of enzyme dissociation constants. J. Am. Chem. Soc. *56*, 658–666.

Luyten, I., and Herdewijn, P. (1998). Hybridization properties of base-modified oligonucleotides within the double and triple helix motif. Eur. J. Med. Chem. *33*, 515–576.

McGuinness, D.H., and McGuinness, D. (2014). m6A RNA Methylation: the implications for health and disease. J. Cancer Sci. Clin. Oncol. *1*, 2394–6520.

Merkestein, M., Laber, S., McMurray, F., Andrew, D., Sachse, G., Sanderson, J., Li, M., Usher, S., Sellayah, D., Ashcroft, F.M., et al. (2015). FTO influences adipogenesis by regulating mitotic clonal expansion. Nat. Commun. *6*, 6792.

Meyer, K.D., Saletore, Y., Zumbo, P., Elemento, O., Mason, C.E., and Jaffrey, S.R. (2012). Comprehensive analysis of mRNA methylation reveals enrichment in 3' UTRs and near stop codons. Cell *149*, 1635–1646.

Neubig, R.R., Spedding, M., Kenakin, T., and Christopoulos, A. (2003). International Union of Pharmacology Committee on Receptor Nomenclature and Drug Classification. XXXVIII. Update on terms and symbols in quantitative pharmacology. Pharmacol. Rev. *55*, 597–606.

Olsen, J.V., Vermeulen, M., Santamaria, A., Kumar, C., Miller, M.L., Jensen, L.J., Gnad, F., Cox, J., Jensen, T.S., Nigg, E.A., et al. (2010). Quantitative phosphoproteomics reveals widespread full phosphorylation site occupancy during mitosis. Sci. Signal. *3*, ra3.

Paige, J.S., Wu, K.Y., and Jaffrey, S.R. (2011). RNA mimics of green fluorescent protein. Science *333*, 642–646.

Paige, J.S., Nguyen-Duc, T., Song, W., and Jaffrey, S.R. (2012). Fluorescence imaging of cellular metabolites with RNA. Science *335*, 1194.

Palamakumbura, A.H., and Trackman, P.C. (2002). A fluorometric assay for detection of lysyl oxidase enzyme activity in biological samples. Anal. Biochem. *300*, 245–251.

Rickardson, L., Fryknäs, M., Haglund, C., Lövborg, H., Nygren, P., Gustafsson, M.G., Isaksson, A., and Larsson, R. (2006). Screening of an annotated compound library for drug activity in a resistant myeloma cell line. Cancer Chemother. Pharmacol. *58*, 749–758.

Rudolf, A.F., Skovgaard, T., Knapp, S., Jensen, L.J., and Berthelsen, J. (2014). A comparison of protein kinases inhibitor screening methods using both enzymatic activity and binding affinity determination. PLoS One *9*, e98800.

Sharma, K., D'Souza, R.C., Tyanova, S., Schaab, C., Wiśniewski, J.R., Cox, J., and Mann, M. (2014). Ultradeep human phosphoproteome reveals a distinct regulatory nature of Tyr and Ser/Thr-based signaling. Cell Rep. *8*, 1583–1594.

Song, W., Strack, R.L., Svensen, N., and Jaffrey, S.R. (2014). Plug-and-play fluorophores extend the spectral properties of spinach. J. Am. Chem. Soc. *136*, 1198–1201.

Umeda, N., Suzuki, T., Yukawa, M., Ohya, Y., Shindo, H., Watanabe, K., and Suzuki, T. (2005). Mitochondria-specific RNA-modifying enzymes responsible for the biosynthesis of the wobble base in mitochondrial tRNAs. Implications for the molecular pathogenesis of human mitochondrial diseases. J. Biol. Chem. *280*, 1613–1624.

Warner, K.D., Chen, M.C., Song, W., Strack, R.L., Thorn, A., Jaffrey, S.R., and Ferré-D'Amaré, A.R. (2014). Structural basis for activity of highly efficient RNA mimics of green fluorescent protein. Nat. Struct. Mol. Biol. *21*, 658–663.

Zhang, J.H., Chung, T.D.Y., and Oldenburg, K.R. (1999). A simple statistical parameter for use in evaluation and validation of high throughput screening assays. J. Biomol. Screen. *4*, 67–73.